Finally, as a stronger external perturbation in general would lead to a larger band repulsion, a rope could behave like a semiconductor under a sufficiently strong perturbation. This may be an explanation for the quantum dot behaviour of isolated tubes and ropes[7,8] in which some semiconductor barrier region seemingly develops at the contact where a substantial perturbation in potential is expected to occur. □

Received 23 July; accepted 17 November 1997.

1. Iijima, S. Helical microtubules of graphitic carbon. *Nature* **354,** 56–58 (1991).
2. Thess, A. *et al.* Crystalline ropes of metallic carbon nanotubes. *Science* **273,** 483–487 (1996).
3. Cowley, J. M., Nikolaev, P., Thess, A. & Smalley, R. E. Electron nano-diffraction study of carbon single-walled nanotube ropes. *Chem. Phys. Lett.* **265,** 379–384 (1997).
4. Hamada, N., Sawada, S. & Oshiyama, A. New one-dimensional conductors: graphitic microtubules. *Phys. Rev. Lett.* **68,** 1579–1581 (1992).
5. Mintmire, J. W., Dunlap, B. I. & White, C. T. Are fullerene tubules metallic? *Phys. Rev. Lett.* **68,** 631–634 (1992).
6. Saito, R., Fujita, M., Dresselhaus, G. & Dresselhaus, M. S. Electronic structure of chiral graphene tubules. *Appl. Phys. Lett.* **60,** 2204–2206 (1992).
7. Tans, S. J. *et al.* Individual single-wall carbon nanotubes as quantum wires. *Nature* **386,** 474–477 (1997).
8. Bockrath, M. *et al.* Single-electron transport in ropes of carbon nanotubes. *Science* **275,** 1922–1925 (1997).
9. Krotov, Y. A., Lee, D.-H. & Louie, S. G. Low energy properties of (*n*,*n*) nanotubes. *Phys. Rev. Lett.* **78,** 4245–4248 (1997).
10. Cohen, M. L. & Chelikowsky, J. R. *Electronic Structure and Optical Properties of Semi-conductors*, 20 (Springer, Berlin, 1988).
11. Charlier, J.-C., Gonze, X. & Michenaud, J.-P. First-principles study of the stacking effect on the electronic properties of graphites. *Carbon* **32,** 289–299 (1994).
12. Charlier, J.-C., Gonze, X. & Michenaud, J.-P. First-principles study of carbon nanotube solid-state packings. *Europhys. Lett.* **29,** 43–48 (1995).
13. Song, S. N., Wang, X. K., Chang, R. P. H. & Ketterson, J. B. Electronic properties of graphite nanotubules from galvanomagnetic effects. *Phys. Rev. Lett.* **72,** 697–700 (1994).
14. Langer, L. *et al.* Quantum transport in a multiwalled carbon nanotube. *Phys. Rev. Lett.* **76,** 479–482 (1996).

Acknowledgements. We thank V. Crespi for discussions and for providing relaxed atomic coordinates. This work was supported by the NSF and DOE. P.D. thanks the NUI for support; H.J.C. and J.I. were supported by the BSRI program of the Ministry of Education of Korea and the SRC program of KOSEF; and S.G.L. acknowledges the hospitality of the Aspen Center for Physics.

Correspondence should be addressed to S.G.L. (e-mail: louie@jungle.berkeley.edu).

Recognition of the four Watson–Crick base pairs in the DNA minor groove by synthetic ligands

Sarah White, Jason W. Szewczyk, James M. Turner, Eldon E. Baird & Peter B. Dervan

Division of Chemistry and Chemical Engineering and Beckman Institute, California Institute of Technology, Pasadena, California 91125, USA

The design of synthetic ligands that read the information stored in the DNA double helix has been a long-standing goal at the interface of chemistry and biology[1–5]. Cell-permeable small molecules that target predetermined DNA sequences offer a potential approach for the regulation of gene expression[6]. Oligodeoxynucleotides that recognize the major groove of double-helical DNA via triple-helix formation bind to a broad range of sequences with high affinity and specificity[3,4]. Although oligonucleotides and their analogues have been shown to interfere with gene expression[7,8], the triple-helix approach is limited to recognition of purines and suffers from poor cellular uptake. The subsequent development of pairing rules for minor-groove binding polyamides containing pyrrole (Py) and imidazole (Im) amino acids offers a second code to control sequence specificity[9–11]. An Im/Py pair distinguishes G·C from C·G and both of these from A·T/T·A base pairs[9–11]. A Py/Py pair specifies A,T from G,C but does not distinguish A·T from T·A[9–14]. To break this degeneracy, we have added a new aromatic amino acid, 3-hydroxypyrrole (Hp), to the repertoire to test for pairings that discriminate A·T from T·A. We find that replacement of a single hydrogen atom with a hydroxy group in a Hp/Py pairing regulates affinity and specificity by an order of magnitude. By incorporation of this third amino acid, hydroxypyrrole–imidazole–pyrrole polyamides form four ring-pairings (Im/Py, Py/Im, Hp/Py and Py/Hp) which distinguish all four Watson–Crick base pairs in the minor groove of DNA.

Because of the degeneracy of the hydrogen-bond donors and acceptors displayed on the edges of the base pairs, the minor groove was thought to lack sufficient information for a complete recognition code[15]. But, despite the central placement of the guanine exocyclic N2 amine group in the G,C minor groove[15,16], Py/Im and Im/Py pairings distinguish energetically between G·C and C·G[9–11,17,18]. The neighbouring Py packs an Im to one side of the minor groove resulting in a precisely placed hydrogen bond between Im N3 and guanine N2 for specific recognition[19,20]. This remarkable sensitivity to single atomic replacement indicates that substitution at the 3 position of one Py within a Py/Py pair can complement small structural differences at the edges of the base pairs in the centre of the minor groove. For A,T base pairs, the hydrogen-bond acceptors at N3 of adenine and O2 of thymine are almost identically placed in the minor groove, making hydrogen-bond discrimination a challenge (Fig. 1)[15]. The existence of an asymmetrically placed cleft on the minor groove surface between the thymine O2 and the adenine 2H suggests a possible shape-selective mechanism for A·T recognition[21]. We reasoned that substitution of C3–H by C3–OH within a Py/Py pair would create 3-hydroxypyrrole (Hp)/Py pairings to discriminate T·A from A·T (Fig. 2). Selectivity could potentially arise from steric destabilization of polyamide binding via placement of Hp opposite A or stabilization by specific hydrogen bonds between Hp and T.

Four-ring polyamide subunits, covalently coupled to form eight-ring hairpin structures, bind specifically to 6-base-pair (bp) target sequences at subnanomolar concentrations[11,18]. We report here the DNA-binding affinities of three eight-ring hairpin polyamides containing pairings of Im/Py, Py/Im opposite G·C, C·G and either Py/Py, Hp/Py or Py/Hp at a common single point opposite T·A and A·T (Fig. 2b). Equilibrium dissociation constants (K_D) for ImImPyPy-γ-ImPyPyPy-β-Dp (**1**), ImImPyPy-γ-ImHpPyPy-β-Dp (**2**), and ImImHpPy-γ-ImPyPyPy-β-Dp (**3**) were determined by

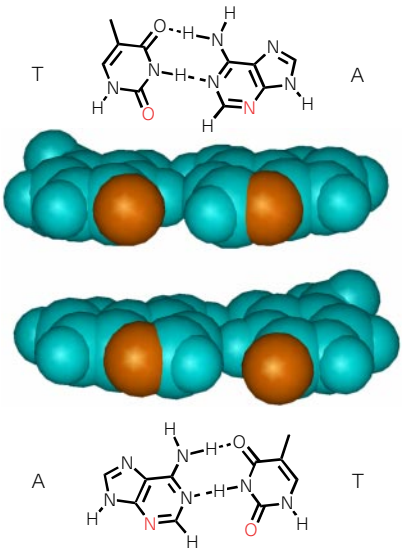

Figure 1 Chemical structures and space-filling models of the T·A and A·T base pairs as viewed from the minor groove of DNA. Models generated using B-form DNA coordinates provided in InsightII. The hydrogen-bond acceptors (N3 of adenine and O2 of thymine) are in red.

Table 1 Equilibrium dissociation constants

	K_D (nM)		
Polyamide*	5′-TGGTCA-3′	5′-TGGACA-3′	K_{rel}†
1 Py/Py	0.077	0.15	2.0
2 Py/Hp	15	0.83	0.06
3 Hp/Py	0.48	37	77

The reported dissociation constants are the average values obtained from three DNase I footprint titration experiments. The standard deviation for each data set is less than 15% of the reported number. Assays were carried out in the presence of 10 mM Tris·HCl, 10 mM KCl, 10 mM $MgCl_2$ and 5 mM $CaCl_2$ at pH 7.0 and 22 °C.
* Ring pairing opposite T·A and A·T in the fourth position.
† Calculated as K_D(5′-TGGACA-3′)/K_D(5′-TGGTCA-3′).

Table 2 Pairing code for minor groove recognition

Pair	G·C	C·G	T·A	A·T
Im/Py	+	–	–	–
Py/Im	–	+	–	–
Hp/Py	–	–	+	–
Py/Hp	–	–	–	+

Favoured (+), disfavoured (–).

quantitative DNase I footprint titration experiments[22] on a 3′ ^{32}P-labelled 250-bp DNA fragment containing the target sites, 5′-TGGACA-3′ and 5′-TGGTCA-3′ which differ by a single A,T base pair in the fourth position (Fig. 3, Table 1).

Based on the pairing rules for polyamide-DNA complexes both of these sequences are a match for control polyamide **1** which places a Py/Py pairing opposite A·T and T·A at both sites. We find that polyamide **1** (Py/Py) binds to 5′-TGGTCA-3′ and 5′-TGGACA-3′ within a factor of 2 ($K_D = 0.077$ or 0.15 nM respectively). In contrast, polyamide **2** (Py/Hp) binds to 5′-TGGTCA-3′ and 5′-TGGACA-3′ with dissociation constants that differ by a factor of 18 ($K_D = 15$ nM and 0.83 nM respectively). If the pairing is reversed in polyamide **3** (Hp/Py) the dissociation constants differ again in the opposite direction by a factor of 77 ($K_D = 0.48$ nM and 37 nM respectively). Control experiments on separate DNA fragments[18,23] reveal that neither a 5′-TGGGCA-3′ nor a 5′-TGGCCA-3′ site is bound by polyamide **2** or **3** at concentrations ≤100 nM, indicating that the Hp/Py and Py/Hp ring pairings do not bind opposite G·C or C·G.

The discrimination between A·T and T·A is achieved when the two neighbouring base pairs are G·C and C·G (GTC compared with GAC). A general rule would require that the same discrimination be observed when adjacent A·T/T·A base pairs are present in the target sequence. Further sequence composition studies, which will be reported in due course, confirm A·T/T·A discrimination at sequence contexts which include TTT, TAA, TAT, TTA, ATT, GTT, GAT, and GTA steps (see Supplementary Information).

The specificity of **2** and **3** for sites that differ by a single A·T/T·A base pair results from small chemical changes. Replacing the Py/Py pair in **1** with a Py/Hp pairing as in **2**, a single substitution of C3–OH for C3–H, destabilizes interaction with 5′-TGGTCA-3′ by 191-fold, a free-energy difference of 3.1 kcal mol^{-1} (13.0 kJ mol^{-1}). Interaction of **2** with 5′-TGGACA-3′ is destablized only 6-fold relative to **1**, a free-energy difference of 1.1 kcal mol^{-1} (4.6 kJ mol^{-1}). Similarly,

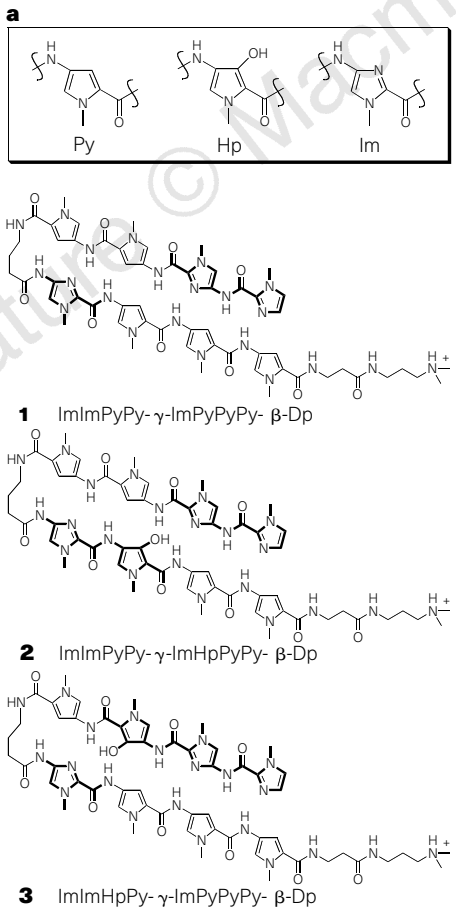

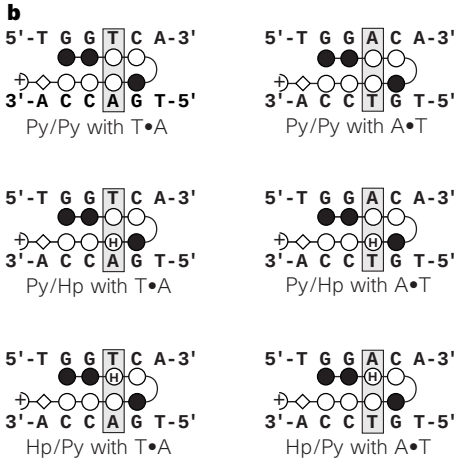

Figure 2 Eight-ring hairpin polyamides containing three aromatic amino acids (Py, Hp, Im). **a**, Structures of polyamides ImImPyPy-γ-ImPyPyPy-β-Dp (**1**), ImImPyPy-γ-ImHpPyPy-β-Dp (**2**), ImImHpPy-γ-ImPyPyPy-β-Dp (**3**). (Hp = 3-hydroxypyrrole, Im = imidazole, Py = pyrrole, β = β-alanine, γ = γ-aminobutyric acid, Dp = dimethylamino-propylamide.) Polyamides were synthesized by solid-phase methods using Boc-protected 3-methoxypyrrole, imidazole and pyrrole aromatic amino acids, cleaved from the support by aminolysis, deprotected with sodium thiophenoxide, (full synthetic detail will be described elsewhere) and purified by reversed-phase high-performance liquid chromatograph (HPLC)[28]. The identity and purity of the polyamides were verified by ^{1}H NMR, analytical HPLC, and matrix-assisted laser-desorption ionization time-of-flight mass spectrometry (MALDI-TOF MS-monoisotopic): **1** 1223.6 (1223.6 calculated); **2** 1239.6 (1239.6 calculated); **3** 1239.6 (1239.6 calculated). **b**, Binding models for polyamide **1**–**3** in complex with 5′-TGGTCA-3′ and 5′-TGGACA-3′ (A·T and T·A in fourth position highlighted). Filled and unfilled circles represent imidazole and pyrrole rings respectively; circles containing an H represent 3-hydroxypyrrole, the curved line connecting the polyamide subunits represents γ-aminobutyric acid, the diamond represents β-alanine, and the + represents the positively charged dimethylaminopropylamide tail group.

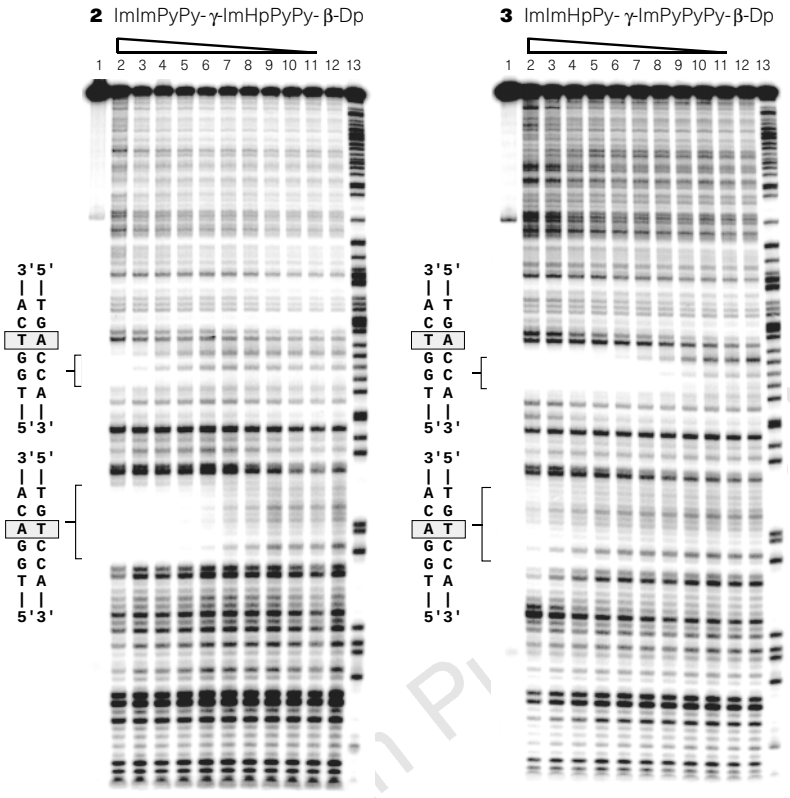

Figure 3 Quantitative DNase I footprint titration experiments. These experiments were made with polyamides **2** and **3** on the 3′ ^{32}P-labelled 250-bp pJK6[29] *Eco*RI/*Pvu*II restriction fragment. Lane 1, intact DNA; lanes 2-11 DNase I digestion products in the presence of 100, 50, 20, 10, 5, 2, 1, 0.5, 0.2, 0.1 nM polyamide, respectively; lane 12, DNase I digestion products in the absence of polyamide; lane 13, adenine-specific chemical sequencing. All reactions were done in a total volume of 400 μl. A polyamide stock solution or H_2O was added to an assay buffer containing radiolabelled restriction fragment, with the final solution conditions of 10 mM Tris-HCl, 10 mM KCl, 10 mM $MgCl_2$, 5 mM $CaCl_2$, pH 7.0. Solutions were allowed to equilibrate for 4–12 h at 22 °C before initiation of footprinting reactions. Footprinting reactions, separation of cleavage products and data analysis were carried out as described previously[13].

replacing the Py/Py pair in **1** with Hp/Py as in **3** destabilizes interaction with 5′-TGGACA-3′ by 252-fold, a free-energy difference of 3.2 kcal mol^{-1}. Interaction of **3** with 5′-TGGTCA-3′ is destabilized only 6-fold relative to **1**, a free-energy difference of 1.0 kcal mol^{-1}. Determining the exact molecular basis for T·A recognition by Hp/Py must await high-resolution X-ray structure studies. For example, there is the possibility that the OH group of Hp is engaged in a hydrogen-bonding interaction with O2 of T.

Molecular recognition in nature occurs through an ensemble of stabilizing and destabilizing forces[16]. For example the DNA-binding transcription factor, TBP, recognizes 5′-TATA-3′ sequences in the DNA minor groove via specific contacts and a large DNA-bend[24]. For DNA-bending proteins such as TBP, practical sequence-specificity can be increased through the sequence-dependent energetics of DNA distortion[25]. Homeodomain proteins recognize target sequences through a combination of specific interactions with both the major and minor grooves[26]. An N-terminal arm recognizes 5′-TAAT-3 sequences in the minor groove such that a single substitution of T·A for A·T reduces binding at 5′-TTAT-3′ by a factor of 7 (ref. 27). However, no single protein structure motif has been identified that provides a general amino acid–base pair code for the minor groove, although there has been remarkable progress with zinc-fingers in the major groove[30]. Polyamides use a single molecular shape to provide for coded targeting of predetermined DNA sequences with affinity and specificity comparable to sequence-specific DNA binding proteins[11]. Hydroxypyrrole–imidazole–pyrrole polyamides complete the minor-groove recognition code using three aromatic amino acids that combine to form four ring pairings (Im/Py, Py/Im, Hp/Py and Py/Hp) which complement the four Watson–Crick base pairs (Table 2). □

Received 29 September; accepted 24 November 1997.

1. Zimmer, C. & Wähnert, U. Nonintercalating DNA-binding ligands: specificty of the interaction and their use as tools in biophysical, biochemical and biological investigations of the genetic material. *Prog. Biophys. Mol. Biol.* **47,** 31–112 (1986).
2. Dervan, P. B. Design of sequence-specific DNA-binding molecules. *Science* **232,** 464–471 (1986).
3. Moser, H. E. & Dervan, P. B. Sequence-specific cleavage of double helical DNA by triple helix formation. *Science* **238,** 645–650 (1987).
4. Thuong, N. T. & Helene, C. Sequence-specific recognition and modification of double-helical DNA by oligonucleotides. *Angew. Chem. Int. Edn Engl.* **32,** 666–690 (1993).
5. Nielsen, P. E. Design of sequence-specific DNA-binding ligands. *Chem. Eur. J.* **3,** 505–508 (1997).
6. Gottesfeld, J. M., Neely, L., Trauger, J. W., Baird, E. E. & Dervan, P. B. Regulation of gene expression by small molecules. *Nature* **387,** 202–205 (1997).
7. Maher, J. L., Dervan, P. B. & Wold, B. Analysis of promoter-specific repression by triple-helical DNA complexes in a eukaryotic cell-free transcription system. *Biochemistry* **31,** 70–81 (1992).
8. Duvalentin, G., Thuong, N. T. & Helene, C. Specific-inhibition of transcription by triple helix-forming oligonucleotides. *Proc. Natl Acad. Sci. USA* **89,** 504–508 (1992).
9. Wade, W. S., Mrksich, M. & Dervan, P. B. Design of peptides that in the minor groove of DNA at 5′-(A,T)G(A,T)C(A,T)-3′ sequences by a dimeric side-by-side motif. *J. Am. Chem. Soc.* **114,** 8783–8794 (1992).
10. Mrksich, M. *et al.* Antiparallel side-by-side motif for sequence specific-recognition in the minor groove of DNA by the designed peptide 1-methylimidazole-2-carboxamidenetropsin. *Proc. Natl Acad. Sci. USA* **89,** 7586–7590 (1992).
11. Trauger, J. W., Baird, E. E. & Dervan, P. B. Recognition of DNA by designed ligands at subnanomolar concentrations. *Nature* **382,** 559–561 (1996).
12. Pelton, J. G. & Wemmer, D. E. Structural characterization of a 2-1 distamycin A-d(CGCAAATTGGC) complex by two-dimensional NMR. *Proc. Natl Acad. Sci. USA* **86,** 5723–5727 (1989).
13. White, S., Baird, E. E. & Dervan, P. B. Effects of the A·T/T·A degeneracy of pyrrole-immidazole polyamide recognition in the minor groove of DNA. *Biochemistry* **35,** 6147–6152 (1996).
14. White, S., Baird, E. E. & Dervan, P. B. On the pairing rules for recognition in the minor groove of DNA by pyrrole-imidazole polyamides. *Chem. Biol.* **4,** 569–578 (1997).
15. Seeman, N. C., Rosenberg, J. M. & Rich, A. Sequence specific recognition of double helical nucleic acids by proteins. *Proc. Natl Acad. Sci. USA* **73,** 804–808 (1976).
16. Steitz, T. A. Structural studies of protein-nucleic acid interaction: the sources of sequence-specific binding. *Quart. Rev. Biophys.* **23,** 203–280 (1990).
17. Mrksich, M. & Dervan, P. B. Recognition in the minor-groove of DNA at 5′-(A,T)GCGC(A,T)-3′ by a 4-ring tripeptide dimer—reversal of the specificity of the natural product distamycin. *J. Am. Chem. Soc.* **117,** 3325–3332 (1995).
18. Swalley, S. E., Baird, E. E. & Dervan, P. B. Discrimination of 5′-GGGG-3′, 5′-GCGC-3′, and 5′-GGCC-3′ sequences in the minor groove of DNA by eight-ring hairpin polyamides. *J. Am. Chem. Soc.* **119,** 6953–6961 (1997).

19. Kielkopf, C. L., Baird, E. E., Dervan, P. B. & Rees, D. C. Structural basis for G·C recognition in the DNA minor groove. *Nature Struct. Biol* (in the press).
20. Pilch, D. S. *et al.* Binding of a hairpin polyamide in the minor-groove of DNA—sequence-specific enthalpic discrimination. *Proc. Natl Acad. Sci. USA* **93,** 8306–8311 (1996).
21. Wong, J. M. & Bateman, E. TBP-DNA interactions in the minor groove discriminate between A:T and T:A base pairs. *Nucl. Acids Res.* **22,** 1890–1896 (1994).
22. Brenowitz, M., Senear, D. F., Shea, M. A. & Ackers, G. K. Quantitative DNase footprint titration—a method for studying protein-DNA interactions. *Methods Enzymol.* **130,** 132–181 (1986).
23. Swalley, S. E., Baird, E. E. & Dervan, P. B. Recognition of a 5′-(A,T)GGG(A,T)$_2$-3′ sequence in the minor groove of DNA by an 8-ring hairpin polyamide. *J. Am. Chem. Soc.* **118,** 8198–8206 (1996).
24. Kim, Y., Geiger, J. H., Hahn, S. & Sigler, P. B. Crystal Structure of a yeast TBP/TATA-box complex. *Nature* **365,** 512–520 (1993).
25. Gartenberg, M. R. & Crothers, D. M. DNA-sequence determinants of CAP-induced bending and protein-binding affinity. *Nature* **333,** 824–829 (1988).
26. Sluka, J. P., Horvath, S. J., Glasgow, A. C., Simon, M. I. & Dervan, P. B. Importance of minor-groove contacts for recognition of DNA by the binding domain of Hin recombinase. *Biochemistry* **29,** 6551–6561 (1990).
27. Ades, S. E. & Sauer, R. T. Specificity of minor-groove and major-groove interactions in a homeodomain-DNA complex. *Biochemistry* **34,** 14601–14608 (1995).
28. Baird, E. E. & Dervan, P. B. Solid phase synthesis of polyamides containing imidazole and pyrrole amino acids. *J. Am. Chem. Soc.* **118,** 6141–6146 (1996).
29. Kelly, J. J., Baird, E. E. & Dervan, P. B. Binding site size limit of the 2:1 pyrrole–imidazole polyamide-DNA motif. *Proc. Natl Acad. Sci. USA* **93,** 6981–6985 (1996).
30. Choo, Y. & Klug, A. Physical basis of a protein–DNA recognition code. *Curr. Opin. Struct. Biol.* **7,** 117–125 (1997).

Supplementary Information is available on *Nature*'s World-Wide Web site (http://www.nature.com) or as paper copy from Mary Sheehan at the London editorial office of *Nature*.

Acknowledgements. We are grateful to the NIH for research support and National Research service Awards to S.W. and J.W.S., to the NSF for a predoctorial fellowship to S.W., to J. Edward Richter for an undergraduate fellowship to J.M.T., and to the HHMI for a predictorial fellowship to E.E.B.

Correspondence and requests for materials should be addressed to P.B.D. (e-mail: dervan@cco.caltech.edu).

A new perspective on the dynamical link between the stratosphere and troposphere

Dana E. Hartley*, Jose T. Villarin*, Robert X. Black* & Christopher A. Davis†

** Georgia Institute of Technology, Atlanta, Georgia 30332-0340, USA*
† National Center for Atmospheric Research, P.O. Box 3000, Boulder, Colorado 80307, USA

Atmospheric processes of tropospheric origin can perturb the stratosphere, but direct feedback in the opposite direction is usually assumed to be negligible, despite the troposphere's sensitivity to changes in the release of wave activity into the stratosphere[1–3]. Here, however, we present evidence that such a feedback exists and can be significant. We find that if the wintertime Arctic polar stratospheric vortex is distorted, either by waves propagating upward from the troposphere[4] or by eastward-travelling stratospheric waves[5,6], then there is a concomitant redistribution of stratospheric potential vorticity which induces perturbations in key meteorological fields in the upper troposphere. The feedback is large despite the much greater mass of the troposphere: it can account for up to half of the geopotential height anomaly at the tropopause. Although the relative strength of the feedback is partly due to a cancellation[7] between contributions to these anomalies from lower altitudes, our results imply that stratospheric dynamics and its feedback on the troposphere are more significant for climate modelling and data assimilation than was previously assumed.

To test for feedbacks from the stratosphere on the troposphere, we use a method known as piecewise potential–vorticity (PV) inversion. PV inversion more generally means the deduction of geopotential anomaly fields (and related fields such as the wind field) from fields of PV anomalies in the atmosphere and potential temperature anomalies at the Earth's surface. The inversion process requires solving a Poisson-like equation, which indicates that the non-local effects are qualitatively similar to the induction of an electric field by electric charge[8,9]. It is a useful aid to understanding atmospheric motions in circumstances where PV evolution is easily characterized. Piecewise PV inversion uses the superposition principle to calculate contributions to the geopotential height anomaly Z' attributable to PV anomalies in certain locations only[10], analogous to calculating the electric fields that are due to only a subset of the total charge distribution.

The superposition principle is linear when the inversion is done on the basis of quasi-geostrophy (QG), and we accordingly use quasi-geostrophic PV[11,12] (hereafter, simply PV) throughout this study. Quasi-geostrophy is based on the assumption that the magnitude of horizontal wind acceleration is smaller than the force due to the Earth's rotation (small Rossby number) and that the vertical stability is approximately uniform along a pressure-altitude. In QG, PV anomalies, q', and geopotential height anomalies, Z', are linearly related by

$$q' = \mathcal{L}(Z') \quad (1)$$

where $\mathcal{L}$ is a linear laplacian-type operator[8]. The linearity of equation (1) allows piecewise PV inversions to be performed unambiguously, as one can linearly superpose the contributions of individual PV anomaly 'pieces' to obtain the total Z' field.

Piecewise PV inversions have been applied in separate studies of tropospheric cyclogenesis[10,13] and the stratospheric polar vortex[11]. The latter research, which focused on how the stratospheric and mesospheric Z' fields are determined, included an exploratory analysis, using no tropospheric data, of the impact of two large stratospheric vortex deformations on the troposphere. Here we present an analysis and quantification of the influence of stratospheric PV anomalies relative to tropospheric PV anomalies in determining Z' in the upper troposphere. (The tropospheric PV anomalies include anomalies at the tropopause level: that is, those along the boundary between the troposphere and stratosphere.) Our study uses meteorological data for the winter of 1992/93 (analysed fields from the United Kingdom Meteorological Office, UKMO[14]) for both the troposphere and stratosphere, and diagnoses a broad range of cases of stratospheric polar vortex distortions, which are often associated with dramatic advective rearrangements of PV and ozone[15,16]. The radiative effects of carbon dioxide, ozone and other greenhouse gases in the stratosphere, along with the breaking of planetary-scale Rossby waves, are responsible for the strong winds and horizontal PV gradients observed at the edge of the vortex[17,18] which, when disturbed, can easily lead to strong advection. Stratospheric vortex distortions can be due to both the vertical propagation of planetary-scale Rossby waves from the

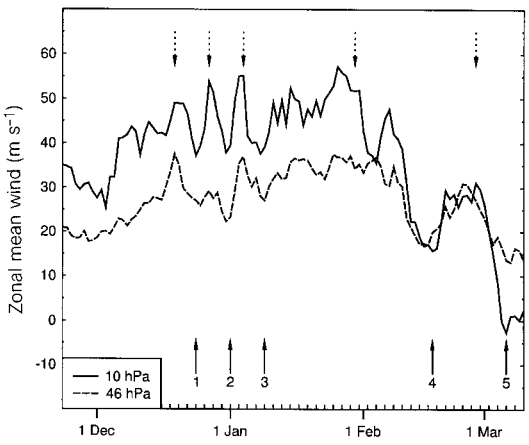

Figure 1 Time series of the zonal mean wind at 61.25° N for the winter of 1992/93. The solid line is for 10 hPa (~30 km) and the dashed line is for 46 hPa (~20 km). Up-arrows mark vortex disturbance events and down-arrows mark non-events. The events are numbered for reference in the text and other figures.